Structural correlates of heterogeneous *in vivo* activity of midbrain dopaminergic neurons

Pablo Henny[1,2,3], **Matthew T C Brown**[1,5], **Augustus Northrop**[1], **Macarena Faunes**[2,3], **Mark A Ungless**[1,5], **Peter J Magill**[1,4], and **J Paul Bolam**[1,4]

[1]MRC Anatomical Neuropharmacology Unit, Department of Pharmacology, University of Oxford, Oxford, UK

[2]Departamento de Anatomía Normal, Escuela de Medicina, Pontificia Universidad Católica de Chile, Santiago, Chile

[3]Centro Interdisciplinario de Neurociencia, NeuroUC, Pontificia Universidad Católica de Chile, Santiago, Chile

[4]Oxford Parkinson's Disease Centre, University of Oxford, Oxford, UK

Abstract

Dopaminergic neurons of the substantia nigra pars compacta (SNc) exhibit functional heterogeneity that likely underpins their diverse roles in behavior. We examined how the functional diversity of identified dopaminergic neurons *in vivo* correlates with differences in somato-dendritic architecture and afferent synaptic organization. Stereological analysis of individually recorded and labeled dopaminergic neurons of rat SNc revealed that they received approximately 8,000 synaptic inputs, at least 30% of which were glutamatergic and 40-70% were GABAergic. The latter synapses were proportionally greater in number and denser on dendrites located in the substantia nigra pars reticulata (SNr) than on those located in SNc, revealing the existence of two synaptically distinct and region-specific subcellular domains. We also found that the relative extension of SNc neuron dendrites into the SNr dictated overall GABAergic innervation and predicted inhibition responses to aversive stimuli. We conclude that diverse wiring patterns determine the heterogeneous activities of midbrain dopaminergic neurons *in vivo*.

Midbrain dopaminergic neurons, including those of the SNc, are important for a variety of brain functions, including voluntary movement and the encoding and prediction of behaviorally relevant stimuli[1,2]. The release of dopamine in their principal target region, the striatum, depends on their firing rate and pattern[2,3], which results from the interactions between the intrinsic membrane properties that endow autonomous pacemaking activity and the synaptic inputs that modify firing in a task- and stimulus-dependent manner[4,5]. Midbrain dopaminergic neurons can encode behaviorally salient events, such as unexpected rewards and aversive stimuli, through phasic increases (bursts) and decreases (pauses) in firing[2,6-10]. Bursting activity is promoted by glutamatergic and cholinergic afferents[4,5], suppressed by GABA[11], and results in transient increases in the release of dopamine in targets[2,3]. Inhibitory responses are mediated by GABAergic afferents[11]. However, not all dopaminergic neurons respond in a specific way to a given stimulus[2], perhaps indicating that subpopulations of neurons are responsive to different stimuli and/or differentially encode the salience, motivational or alerting values of stimuli[6-10]. For instance, in the rat SNc, most dopaminergic neurons are unresponsive to noxious stimuli, but a small proportion is inhibited[7].

We hypothesized that the functional heterogeneity of SNc dopaminergic neurons is a consequence of differences in the architecture and afferent connectivity of their dendrites. Although the wiring diagram of SNc dopaminergic neurons at the population level has been partially elucidated with respect to their multiple inputs[11-16], precise definition of relationships between structure and function necessitates correlative analysis of connectivity at the level of individual identified neurons whose activity has been characterized in intact circuits. We tested our hypothesis by first recording and labeling functionally diverse single SNc neurons *in vivo* and then, after verifying their dopaminergic phenotype, reconstructing their somatodendritic domains and carrying out a stereological analysis at the ultrastructural level of the number and distribution of glutamatergic and GABAergic afferent synapses. Our results establish a direct correlation between dendritic architecture, synaptic innervation and *in vivo* responses to salient stimuli, thus defining the structural substrates underlying the functional heterogeneity of midbrain dopaminergic neurons.

RESULTS

Dendritic architecture of SNc dopaminergic neurons

To correlate the *in vivo* electrophysiological properties with the dendritic architecture and innervation of individual dopaminergic neurons, we extracellularly recorded action potential discharges from single neurons of the substantia nigra (Fig. 1a,b) in anesthetized rats, tested their responses to standardized aversive sensory stimuli (see below) and then juxtacellularly labeled the same neurons with neurobiotin[7,17]. We identified the neurobiotin-labeled neurons as dopaminergic by their expression of the catecholamine synthetic enzyme tyrosine hydroxylase (Fig. 1c–e). Of the dopaminergic neurons located in the SNc (Fig. 1f), we selected those that had complete labeling of their soma and dendrites with the neurobiotin, a condition that was essential to effectively carry out the anatomical analyses. These neurons came from a larger pool of recorded and labeled neurons whose firing characteristics were

recently detailed[7]. The investigators (P.H. and A.N.) were blinded to the electrophysiological characteristics of the neurons during the anatomical analyses.

To examine the dendritic architecture of labeled dopaminergic neurons and facilitate the systematic sampling of their afferent inputs, we digitally reconstructed the cells from serial 50-µm-thick sections under high magnification (Fig. 2a, Online Methods and Supplementary Table 1)[18]. The dendrites of SNc dopaminergic neurons varied in size (length, approximate surface area and number of segments) and complexity (numbers of primary dendrites and highest branch order) (Supplementary Table 1). Moreover, the neurons also varied greatly in the degree to which their dendrites descended into the SNr (ranging from none to over half of total dendritic length; Fig. 2a and Supplementary Table 1; also see ref. 19). Because previous studies have suggested that dopaminergic neurons expressing the calcium-binding protein calbindin have minimal or no extension of dendrites into the SNr[20,21], we further tested for the expression of calbindin immunoreactivity (Supplementary Fig. 1). We found no differences in dendritic size, complexity and relative extension into SNr between calbindin-positive and calbindin-negative dopaminergic neurons ($P > 0.05$, Student's t test; Supplementary Fig. 1). In addition, we found no relation between the dorso-ventral position of the cell bodies in the SNc and either the dendritic size or the proportion of dendrites located in the SNr (data not shown; see ref. 20).

Synaptic innervation of individual dopaminergic neurons

To accurately estimate the number and distribution of synaptic inputs to functionally diverse SNc dopaminergic neurons, we applied stereological methods[22,23] (see Online Methods) to six recorded, labeled, identified and fully reconstructed neurons. We performed systematic random sampling of synapses formed with the dendrites and cell bodies of the labeled neurons and then counted the synapses using a physical fractionator[22], which consisted of a 500-nm-thick dissector located at the upper surface of all sections containing the neurobiotin-labeled processes (see Online Methods and Supplementary Table 2). We found that SNc dopaminergic neurons each formed, on average, ~8,000 afferent synapses (Table 1), 61.8% of which were formed with dendrites located in the SNc and 38.2% with dendrites located in the SNr. The glutamatergic synapses were revealed by immunolabeling of the presynaptic terminals for vesicular glutamate transporter type 2 (VGluT2) in five neurons. In four of these, GABAergic synapses were also revealed by immunolabeling alternate sections for the vesicular GABA transporter (VGAT; Figs. 2b and 3a). The dopaminergic neurons received significantly more GABAergic synaptic inputs (VGAT[+], 50.2% of all synapses, $n = 4$ neurons) than glutamatergic synaptic inputs (VGluT2^{+}, 31.5% of all synapses, $n = 5$ neurons; Student's t test, $P < 0.05$). The remaining 18.3% of synapses were not neurochemically identified, but presumably include glutamatergic (but using a different vesicular transporter[24,25], see below), cholinergic[12] and serotonergic[26] terminals.

We next tested whether the proportions of glutamatergic and GABAergic synapses made with the dendrites of the dopaminergic neurons varied according to whether they were in the SNc or the underlying SNr, two subdivisions of the nigra that receive different afferent innervation[13-15,20,21,27]. We found a significant interaction between the type of synapse and region (vesicular transporter (VGluT2, VGAT) × region (SNc, SNr) as factors, $F_1 = 14.3$, P

< 0.05, two-way ANOVA, $n = 5$ for VGluT2 and $n = 4$ for VGAT). Pairwise multiple comparisons (Student-Newman-Keuls *post hoc* test) revealed that the proportion of glutamatergic synapses was significantly higher on dendrites located in the SNc (35.4%) than on those located in the SNr (20.1%) ($P < 0.05$), that the proportion of GABAergic synapses was higher on dendrites located in the SNr (68.5%) than on those located in the SNc (43.7%) ($P < 0.05$), and that the proportion of GABAergic synapses was significantly higher than that of glutamatergic synapses on dendrites located in the SNr ($P < 0.05$), but not on those located in the SNc ($P > 0.05$) (Fig. 3b and Table 1). These findings indicate that the innervation of dendrites of dopaminergic neurons by neurochemically identified afferents depends on dendrite location (SNc versus SNr), validating earlier qualitative observations at the population level[13].

We further tested whether the relative extension of dendrites of individual neurons into the SNr was a predictor of the overall levels of glutamatergic or GABAergic innervation. There was a significant correlation between the proportion of dendrites located in the SNr and the proportion of synapses that were GABAergic (Pearson's product moment correlation, $R = 0.96$, $P < 0.05$, $n = 4$ neurons; Fig. 3c). In contrast, the proportion of glutamatergic synapses was independent of dendritic extension into the SNr (Pearson's product moment correlation, $R = 0.08$, $P > 0.05$, $n = 5$ neurons; Fig. 3c). These data demonstrate that the proportion of the dendritic field of SNc dopaminergic neurons that extends into the SNr defines the degree of excitatory and inhibitory synaptic afferents that they receive.

Synaptic density in different subcellular domains

Correlative analysis of synaptic innervation with vector-based digital reconstructions of the same neurons[18] allowed us to quantify synaptic densities on different parts of the somato-dendritic tree. We defined proximal dendrites in the SNc as those within 20% of the distance from the cell body to the furthest dendritic tip in the SNc and distal dendrites as those located in the remaining 80% (Fig. 4a, see Online Methods for criteria). We pooled all SNr dendrites into a single group because, according to the same definition used for SNc dendrites, almost all SNr dendrites were located distally (Online Methods and Fig. 4a). We precisely localized each randomly sampled synapse (VGluT2$^+$, VGluT2$^-$, VGAT$^+$, VGAT$^-$, unidentified) along the somato-dendritic membrane and used a Sholl analysis to extract data for the estimated synapse number and approximate surface area of the neuron. With these data, we estimated values for absolute (Table 2) and relative (Fig. 4b,c) synaptic densities for the proximal, distal and SNr dendritic compartments (see Online Methods).

Synaptic density was higher on dendrites located in the SNr than on proximal or distal dendritic compartments located in the SNc (one-way ANOVA, $F_2 = 4.3$, $P < 0.05$; pairwise comparisons, $P < 0.05$; $n = 5$ neurons, Student-Newman-Keuls *post hoc* test; Fig. 4b). These differences were a result of a denser GABAergic innervation of dendrites in SNr compared with proximal or distal dendrites in SNc (Fig. 4c). In contrast, the density of glutamatergic synapses was similar in SNc proximal dendrites, SNc distal dendrites and SNr dendrites (two-way ANOVA, significant interaction for vesicular transporters (VGluT2, VGAT) and region (proximal, distal, SNr) factors, $F = 4.3$, $P < 0.05$; pairwise comparisons, $P < 0.05$ for SNr versus proximal SNc, SNr versus distal SNc within VGAT, and VGluT2 versus VGAT

within SNr, $n = 5$ for VGluT2 and $n = 4$ for VGAT; Fig. 4c). Because the densities of innervation of proximal SNc and distal SNc dendrites were similar, it is likely that the region in which dendrites are located (SNc versus SNr) is the main determinant of the composition and densities of glutamatergic and GABAergic synapses, rather than distance from the cell body *per se*.

Glutamatergic and GABAergic innervation of SNc and SNr

To further define the rules that govern the synaptic innervation of these two subcellular compartments, we quantified the overall proportions of glutamatergic and GABAergic synapses and varicosities in the SNc and SNr and compared them with those forming synaptic contacts with the identified dopaminergic neurons. First, we quantified the proportion of VGluT2^{+} and VGAT[+] synapses in the immediate vicinity of the labeled dopaminergic neurons and dendrites using the stacks of serial electron micrographs that were used to define their afferent input (see Online Methods). There was no significant difference between the proportions of VGAT[+] (40.5 ± 7.6% of total synapses, mean ± s.e.m.) and VGluT2^{+} (33.1 ± 0.3%) synapses made on unlabeled dendrites in the SNc, but there were significantly more VGAT[+] (50.6 ± 5.3%) than VGluT2^{+} (28.8 ± 3.4%) synapses in the SNr (two-way ANOVA with transporters and regions as factors, $F = 9.4$, $P < 0.05$; Student-Neuman-Keuls *post hoc* test, $P < 0.05$ for pairwise significant comparisons, $n = 3$). Second, we performed a systematic random sampling of VGAT[+], VGluT2^{+} and VGluT1^{+} varicosities in the SNc and SNr at the light microscopic level (Supplementary Fig. 2 and Online Methods). We included VGluT1^{+} varicosities in this analysis to give an indication of the proportion of the unlabeled terminals in our electron microscopic analysis that were glutamatergic. As in the ultrastructural analysis, we found no difference between the proportions (percent of all labeled varicosities) of VGAT[+] (55.3 ± 5.5%) and VGluT2^{+} (40.6 ± 5.6%) varicosities in SNc, although the proportion of VGAT[+] varicosities was significantly larger than the proportion of VGluT1^{+} (4.0 ± 1.0%) varicosities. Consistent with the ultrastructural analysis, the proportion of VGAT[+] (70.1 ± 2.8%) varicosities was significantly larger than the proportion of VGluT2^{+} (29.1 ± 2.9%) varicosities in the SNr, as were the differences between the VGAT[+] and VGluT1^{+} varicosities (0.8 ± 2.0%), and between the VGluT2^{+} and VGluT1^{+} varicosities (each value is the mean ± s.e.m.; two-way repeated-measures ANOVA with vesicular transporters and regions as factors, $F = 21.6$, $P < 0.05$; Student-Neuman-Keuls *post hoc* test, $P < 0.05$ for pairwise significant comparisons, $n = 3$).

These ultrastructural and light microscopic analyses indicate that the somato-dendritic domains of SNc dopamine neurons in the SNc and SNr receive afferent synaptic input that reflects the synaptic environment in which they are located, at least with respect to GABAergic and glutamatergic inputs. The light microscopic analysis also revealed that VGluT1^{+} varicosities only account for a small proportion of all of the GABAergic and glutamatergic synapses in both the SNc (4%) and SNr (0.8%), indicating that this class of glutamatergic afferents has a relatively minor contribution to the overall glutamatergic innervation of the substantia nigra and probably also the innervation of individual dopaminergic neurons.

Responses to aversive stimuli correlate with structure

Previously, we found that most identified SNc dopaminergic neurons have no response during aversive stimuli (a pinch applied to the hind paw), whereas a small proportion is inhibited[7]. We asked whether this heterogeneity is a consequence of differences in dendritic architecture and, thus, synaptic input (Fig. 5). We retrospectively analyzed the responses of our anatomically characterized neurons ($n = 11$) to aversive stimuli and divided them into those that were significantly inhibited and those that showed no response, according to previously established criteria based on mean firing rate[7] (see Online Methods). This was possible because none of the SNc neurons were excited according to our criteria, as shown in our previous studies[7]. The neurons inhibited by the stimuli had, on average, a larger proportion of their dendrites extending into the SNr than neurons that did not respond (Student's t test, $P < 0.05$, $n = 5$ neurons for inhibition group and $n = 6$ for no response group; Fig. 5b,c).

Consistent with our finding that the proportion of GABAergic synapses relates to the proportion of the dendritic field in the SNr, the mean proportion of GABAergic synapses in contact with inhibited neurons was higher than that of neurons that did not respond (ratio of VGAT synapses to total number of synapses = 0.67 and 0.54 for two inhibited neurons (mean = 0.61), and 0.4 for two neurons showing no response; Fig. 5d), whereas the mean proportion of glutamatergic synapses was similar between the two groups (ratio of VGluT2 synapses to total number of synapses = 0.32, 0.31 and 0.31 for three inhibited neurons, and 0.26 and 0.38 (mean = 0.32) for two neurons showing no response). There was no difference between the two groups of neurons in terms of the total dendritic length (Student's t test, $P > 0.05$, $n = 11$ neurons; Fig. 5e) and the number of dendritic segments (45.0 ± 10.3 for inhibited versus 57.3 ± 8.8 for nonresponsive neurons, Student's t test, $P > 0.05$, $n = 11$ neurons). Moreover, the mean baseline firing rates of inhibited and nonresponsive neurons were similar (3.6 ± 1.0 Hz for inhibited versus 2.9 ± 0.3 Hz for nonresponsive neurons; Student's t test, $P > 0.05$, $n = 11$ neurons), and baseline firing rates were not correlated with the proportions of dendrites extending into the SNr ($R = 0.22$, $P > 0.05$, Pearson's product moment correlation, $n = 11$ neurons).

To further characterize the relationship between functional properties and morphological characteristics, we tested for a correlation between the proportional change in firing rate in response to the stimulus and the proportion of dendrites extending into the SNr (Fig. 5f). This analysis included both decreases and increases in firing, irrespective of whether they reached the statistical criteria that we previously used to define the responsiveness of neurons[7] (Fig. 5c-e). A larger proportion of dendrites located in the SNr was associated with larger reductions in firing rate (inhibition) during stimulation ($R = -0.52$, $P = 0.052$, Pearson's product moment correlation, $n = 11$ neurons). Together, these data indicate that the relative extension of SNc neuron dendrites into the SNr not only dictates overall GABAergic innervation (Fig. 3c) and the likelihood of neurons being inhibited (Fig. 5c), but also determines the magnitude of the change in activity in response to aversive stimuli (Fig. 5f).

DISCUSSION

We tested the hypothesis that the heterogeneity in the responses of individual dopaminergic neurons to behaviorally relevant stimuli[6-10] is a consequence of differences in dendritic architecture and glutamatergic and GABAergic synaptic innervation. Our analyses revealed that the likelihood of a dopaminergic neuron being inhibited by aversive stimuli, as well as the magnitude of such inhibition, correlates with the proportion of the dendrites located in the SNr, where they receive a higher proportion of GABAergic inputs. Our findings thus provide a structural basis for the diversity of the functional properties of SNc dopaminergic neurons *in vivo*.

Our finding that at least ~30% of presynaptic terminals are glutamatergic (VGluT2$^+$) and that ~50% are GABAergic is supported by previous immunohistochemical studies of putative glutamatergic and GABAergic terminals in synaptic contact with dopaminergic processes in the substantia nigra[13,15]. We also found that about one fifth of synaptic terminals were neither GABAergic nor VGluT2$^+$. Only a small proportion of these were VGluT1$^+$ (4.0% in SNc and 0.8% in SNr of all of the GABAergic and glutamatergic terminals), which are presumably of cortical origin[24,25], suggesting that this remainder must also include cholinergic terminals from mesopontine tegmentum[12,14] and serotonergic terminals from raphe nuclei[26].

Our single-cell analyses revealed that the proportions of glutamatergic and GABAergic afferent synapses vary throughout the somatodendritic domain of a dopaminergic neuron. Thus, we found that glutamatergic synapses were more numerous on the dendrites and perikaryon located in the SNc than on those located in the SNr (~35% of synapses in the SNc versus ~20% of those in SNr), which may be explained by a lower proportion of GABAergic synapses on SNc dendrites. In contrast, a higher proportion of GABAergic synapses was found on dendrites located in the SNr (~43% of synapses in the SNc versus ~69% of those in SNr), where they were more densely packed, as had been suggested in earlier qualitative analyses[13]. Notably, these proportions reflect the overall proportions of glutamatergic and GABAergic synapses in the SNc and SNr, suggesting that innervation of dopaminergic neuron dendrites is more region specific than cell specific. This supports the notion that the dendrites of SNc dopaminergic neurons that penetrate the SNr define an additional subcellular compartment with different synaptic inputs and different rules of connectivity (Supplementary Fig. 3).

By being proportionally more numerous and closer to the axon initial segment (located at the soma or a proximal dendrite[4]), glutamatergic inputs to SNc-located processes may be better suited to drive the activity of dopaminergic neurons than glutamatergic inputs to SNr-located dendrites of the same neurons. Presumably, the efficacy of glutamatergic inputs to SNr dendrites would be further reduced by local interaction with the more numerous GABAergic synapses acting on these dendrites[28,29]. Our finding that neurons with a smaller proportion of dendrites in the SNr have smaller reductions in activity in response to the aversive stimuli supports this notion. We also found that the approximate densities of glutamatergic synapses did not differ between proximal and distal dendrites in the SNc. Thus, glutamatergic synapses targeting proximal regions may be more effective at driving

the activity of dopaminergic neurons[4], provided that there are no mechanisms in distal dendrites actively scaling up synaptic efficacy[30]. The functional relevance of two dendritic compartments (SNc versus SNr) is further emphasized when considering the segregation of glutamatergic inputs in SNc and SNr. Afferents from the superior colliculus[31] and mesopontine tegmentum[14], which preferentially target SNc and contain neurons expressing VGluT2 (refs. 32,33), are theoretically in a better position to drive dopaminergic neurons than afferents from the glutamatergic subthalamic nucleus[34] that favor the SNr[27].

The synaptic organization of functionally distinct dopaminergic neurons also sheds lights on the mechanisms that mediate inhibition of firing. Given the higher number, ratio and density of GABAergic inputs to SNr dendrites, inhibitory synapses on dendrites located in the SNr may be more effective at hyperpolarizing or shunting the membrane potential than synapses made with dendrites located in the SNc, thereby allowing distal SNr dendrites to mediate inhibition. Indeed, our results provide structural evidence supporting previous findings that electrical stimulation of SNr is more efficient at eliciting monosynaptic inhibitory postsynaptic potentials in dopaminergic neurons than stimulation in the SNc itself[35]. The lower number, ratio and density of GABAergic synapses that we observed in proximal regions (that is, in the SNc), unlike the innervation of cortical pyramidal cells[36,37], SNr or pallidal neurons[16], may also explain the comparatively lower efficacy of inhibition by GABA of dopaminergic neurons[38,39]. The multiple GABAergic inputs to the substantia nigra (which include those arising in basal ganglia nuclei[13,16,40] that preferentially target the SNr), the rostromedial tegmentum (which preferentially targets the SNc[41]) and the local collaterals of SNr neurons (which innervate both nigral regions[42]) may inhibit dopaminergic neurons[40,41,43] through parallel actions in these two dendritic compartments.

Our results establish a direct correlation between the dendritic architecture, synaptic innervation and *in vivo* firing of identified midbrain dopaminergic neurons. These new rules of connectivity have important functional implications. The inhibitory responses of SNc dopaminergic neurons, which, by transiently decreasing dopamine release, contribute to signaling, encoding and learning of non-favorable behavioral contingencies[2,6-10], are related to the relative length of dendrites in the SNr and therefore overall GABAergic innervation. For SNc dopaminergic neurons with dendrites in the SNr, it is tempting to speculate that inhibition is facilitated by the concerted action of brainstem structures innervating the SNc[41,44] and of basal ganglia nuclei (striatum, pallidum, SNr)[40], through which the cortex and other high-order forebrain structures may exert a top down control over the their activity[45]. Inhibition of dopaminergic neurons with most of their dendrites in the SNc may be limited to the action of fewer regions, which would include those brainstem structures related to processing and relay of ascending somato-sensory inputs (bottom up control)[44]. Thus, one might conjecture that functional diversity in dopaminergic neurons is a reflection of a differential degree of forebrain control over their activity. A dual forebrain and brainstem influence may be also be seen as an important factor in facilitating inhibition, as we previously found that dopaminergic neurons in SNr, whose somata and entire dendritic field were located in the SNr, were no more likely to be inhibited than SNc neurons[7]. The structural determinants of activity that we describe here are probably relevant to other

neurons, including ventral tegmental area dopaminergic neurons, whose diverse functional properties may relate to different degrees or patterns of GABAergic innervation[46].

ONLINE METHODS

Experimental procedures were performed on adult male Sprague-Dawley rats (Charles River or from facilities at the Pontificia Universidad Católica de Chile) and in accordance with the UK Animals (Scientific Procedures) Act, 1986, and guidelines of the Committee for Ethics and Welfare of Animals (CEBA-MedUC).

Extracellular recording and juxtacellular labeling

Unless specified, procedures were carried out as described previously[7]. Anesthesia was induced with isofluorane (Isoflo, Schering-Plough) and maintained with urethane (1.3 g per kg of body weight, intraperitoneal, ethyl carbamate, Sigma) and a mixture of ketamine (30 mg per kg, intraperitoneal, Ketaset, Willows Francis) and xylazine (3 mg per kg, intraperitoneal, Rompun, Bayer). Epidural electrocorticogram was recorded from motor cortex to monitor spontaneous and driven brain states[7]. Extracellular recordings of single-unit activity were made using glass electrodes (~1.5-μm tip diameter, 10–25 MΩ) containing 0.5 M NaCl and 1.5% neurobiotin (wt/vol, Vector Laboratories). Stereotaxic coordinates were derived from ref. 47. Responses of putative dopaminergic neurons to somato-sensory stimulation were tested by 15-s pinches of the hind paw using pneumatically driven forceps[7]. Following the recordings, the same neurons were labeled by the juxtacellular method[7]. After 2–12 h, the rats were perfuse-fixed with ~100 ml of phosphate-buffered saline (PBS, pH 7.4), followed by 300 ml of 0.1% glutaraldehyde (wt/vol) and 4% paraformaldehyde (wt/vol) in phosphate buffer (pH 7.4), and then ~100 ml of PBS.

For quantification, baseline spontaneous firing was recorded for 30 s immediately preceding the pinch and compared with the activity during the pinch. Firing rate was plotted against time (1-s bins); a neuron was defined as being significantly responsive if two consecutive histogram bins (in the 15-s stimulus period) lay outside 2 s.d. from the baseline mean rate. To ensure that the absence of significant responses to a pinch was not a result of excessively deep anesthesia, activation of the electrocorticogram in response to the pinch was confirmed[7]. Changes in response to the pinch were further characterized (see Fig. 5f) by calculating the mean changes in firing rate in response to consecutive (1 to 7) pinches (percentage change = $[(FR_{Post} - FR_{Pre})/FR_{Pre}] \times 100$; FR_{Pre} = mean spontaneous firing rate immediately preceding the pinches, 30 s; FR_{Post} = mean firing rate during the pinches, 15 s).

Neurons processed and analyzed, and special cases

Neurons were selected for study at the time of the fluorescence labeling used to confirm the presence of tyrosine hydroxylase immunoreactivity (see below) and/or after permanent labeling (see below). The first neuron analyzed was recorded and labeled under isofluorane anesthesia and only the anatomical analyses (at the light and electron microscopy level) were performed. As the project and the method evolved (including the systematic use of urethane for electrophysiological analysis, as described above), we included immunolabeling of presynaptic terminals. Initially, we immunolabeled all of the sections of

one neuron for VGluT2 and then alternate sections of four neurons for VGluT2 and VGAT. In the neurons analyzed at the electron microscopy level, an average of 79 synapses were counted per neuron (Supplementary Table 2). Six additional electrophysiologically characterized dopaminergic neurons were reconstructed and analyzed at the light microscopy level only. We thus examined 12 neurons at the light microscopy level; six of these were subjected to the detailed electron microscopy analysis, of which one was only stained to reveal the neuron (and not analyzed electrophysiologically, see above), one was also immunostained for VGluT2, and four were immunostained for both VGluT2 and VGAT.

Fluorescent immunolabeling for neurochemical identity

The brains were cut in the parasagittal plane on a vibrating microtome (Leica) at 50 μm. The first section was cut at a random thickness (between 1 to 50 μm) to ensure random sampling[22]. Sections containing the substantia nigra were incubated overnight in Cy3-conjugated streptavidin (1:1,000, Zymed) to reveal the neurobiotin. The sections were examined in an epifluorescent (Leica microsystems) or laser-scanning confocal (Zeiss) microscope. Sections containing the cell body and/or thick primary dendrites were selected, blocked in 10% normal donkey serum (NDS, vol/vol, Jackson Immunoresearch), and incubated with mouse antibody to tyrosine hydroxylase (1:1,000, Sigma) and goat antibody to calbindin (1:500, Santa Cruz Biotechnology) in 1% NDS PBS. They were then incubated in AlexaFluor488-conjugated donkey antibody to mouse IgG or goat IgG (1:1,000, Invitrogen), and Cy5-conjugated donkey antibody to mouse IgG or goat IgG (1:1,000, Jackson Immunoresearch) and mounted. AlexaFluor488 fluorescence was imaged with excitation from an argon 488-nm laser, with emission restricted by a BP 510–530 filter. Cy3 fluorescence was imaged with excitation from a helium/neon 543-nm laser, with emission restricted by a LP 560 filter (for the shorter wavelengths) and a NFT 635 VIS 2° dichroic (for longer wavelengths). Cy5 fluorescence was imaged with excitation from a helium/neon 633-nm laser, with emission restricted by either a LP 650 filter. Labeling for neurobiotin and colocalization with calbindin and tyrosine hydroxylase was assessed. In cases where staining was not clear, the sections were freeze-thawed (see ref. 48) and the processing repeated. Only neurochemically identified (tyrosine hydroxylase expressing) SNc dopaminergic neurons were analyzed.

Permanent labeling

Neurons that were strongly labeled with neurobiotin were selected (blind to electrophysiological phenotype) and processed for permanent, peroxidase labeling. Sections were freeze-thawed[48] and then incubated in avidinbiotin peroxidase complex (ABC Elite, 1:100, Vector) to reveal the neurobiotin, together with rabbit antibodies to VGluT2 (1:2,000, Synaptic Systems) or VGAT (1:500, Synaptic Systems) in alternate sections. For one neuron, all sections were incubated with antibody to VGluT2. They were then incubated with donkey antibody to rabbit IgG (1:100, Jackson) for a subsequent peroxidase-anti-peroxidase (PAP) reaction. After washing, the sections were incubated in Tris buffer (0.05 M, pH 7.6) containing 0.002% H_2O_2 (wt/vol, Sigma), 0.025% diaminobenzidine tetrahydrochloride (DAB, wt/vol, Sigma) and 0.5% nickel ammonium sulfate (wt/vol, Sigma). This labeled neurobiotin-filled neurons with a blue/black precipitate (see Fig. 2b).

The sections were then incubated with rabbit PAP (1:100 dilution, Jackson) and the DAB procedure was repeated, but without nickel. This resulted in VGluT2- or VGAT-immunoreactive axon terminals labeled by a brown precipitate (see Fig. 2b). The sections were then post-fixed in 1% osmium tetroxide (wt/vol in PBS, pH 7.4, Oxkem, including 5% β-D-glucose), dehydrated, infiltrated with resin (Durcupan ACM, Fluka), mounted on slides and cured at 60 °C for 70 h[48].

Digital reconstructions

All digitally reconstructed neurons were completely filled; all of the dendrites extended to natural tapering ends and none faded away, and axons were traced for long distances (up to the internal capsule). They were digitally reconstructed in three dimensions using Neurolucida (MicroBrightField), a Nikon Eclipse microscope (100× objective) equipped with an *x, y, z* motor stage and Lucivid (MicroBrightField). Neuronal fragments from every section were traced onto a corresponding digital section using the Serial Section Manager in Neurolucida. High-(100× objective) and low-magnification (2× and/or 10× objectives) images were acquired at the top of each section to assist the electron microscopy analysis (see below). Contours of the SNc and SNr were drawn at lower magnification. After all processes and contours were traced in each individual digital section, a copy of the file (the unspliced file) was saved to assist subsequent sampling of synapses in Stereo Investigator (MicroBrightField). A second copy of the file was used to produce full neuron reconstructions (see Figs. 2a and 5b) through splicing of corresponding dendritic fragments (the spliced file). A shrinkage correction factor was applied to the *x* (6.3%), *y* (6.0%) and *z* (8.0%) dimensions[49]. Quantitative data for anatomical parameters were obtained using the Neurolucida Explorer software.

Re-embedding and acquisition of images

Tissue pieces containing dendritic (or cell body) segments were cut out of the sections and re-embedded for ultrathin sectioning. Blocks were produced for all dendritic or cell body fragments located at the top of every section. Series of ultrathin sections (50 nm, at least ten per single-slot grid) were cut on an ultramicrotome (Leica Microsystems, EM UC6) and contrasted in lead citrate[48]. Sections were examined in an electron microscope (Philips CM100) and fragments of dendrites (or cell body) were identified. Electron micrographs were acquired of the labeled structures in each ultrathin section (UltraScan 1000 CCD camera, Gatan). Given the random and systematic nature of the analysis, which quantifies only synapses that are located at the upper surface of 50 μm of the sections, we did not always have access to the cell body or the axon initial segment. They were not analyzed separately, but were included in the proximal region of neurons.

Offline counting of synapses

The unspliced file copy of the digital reconstruction of each section was opened in Stereo Investigator, where the optical fractionator probe was set up. Using the workflow option, a counting frame of equal size to the sampling grid was set up so as to sample all dendritic/cell body fragments. The dissector height (or sampling region at the top of the section) was set to 0.5 μm (corresponding to 10×50 nm ultrathin sections). Block advance (50 μm) and

mounted section thickness (46 μm as a result of shrinkage[49]) were specified. In each fractionator probe, stacks of serial images were loaded at the exact magnification and location of the corresponding traced dendritic fragment/cell body. Only the 'tops' of synapses were counted[22]. A synapse was identified by the presence of presynaptic vesicles, flattening of the opposed membranes, synaptic cleft and cleft material. Synaptic boutons were defined as VGluT2+, VGAT+, unlabeled (VGluT2- and VGAT-) or unidentified (Fig. 3). The procedure was repeated for all of the traced neuronal fragments. The total number of synapses of individual neurons was then estimated. This was computed by dividing the number of counted markers by the height sampling fraction (0.5 μm/46 μm = 0.01087 for quantification of all synapses or 0.5 μm/92 μm = 0.00543 for quantification of synapses in VGluT2 or VGAT series).

Distribution and density of synapses across dendrites

Each dendrite was classified as located in SNc or SNr. For SNc dendrites, they were defined as proximal when located within a distance equivalent to 20% of the longest possible distance from the cell body to any dendrite tip in the SNc. Proximal SNc regions included ~66% of primary dendritic length and only ~3% of the highest order (5–8° branch order) dendritic length. Conversely, proximal dendritic length consisted of ~23% primary dendrites (68% primary and secondary dendrites) and only ~1% from highest order dendrites. Almost all of the dendrites in SNr (~95% SNr dendritic length) were distal and were therefore pooled into one group: SNr. The 20%/80% criterion separates the neuron into compartments of approximately similar size in terms of surface and number of synapses, allowing one to carry out statistical analyses. In Neurolucida, markers of the different synapses were placed in the exact location from which they were sampled. A Sholl analysis was performed on the spliced file with the different synapses assigned to proximal or distal SNc dendrites or to SNr dendrites. Estimates of number of synapses in each compartment were then combined with approximate length or approximate surface area for the same compartments to estimate synaptic density.

Proportions of synapses on unlabeled dendrites in SNc and SNr

The stacks of electron micrographs used for stereological analysis of individual neurons (see above) were used to count synapses on unlabeled dendrites located in the immediate vicinity of the labeled dopaminergic dendrites (up to ~2.8 μm from the labeled structures, that is, maximum distance from the center of a 4.0 × 4.0 μm micrograph to an edge). Proportions of immunopositive synapses are expressed as percentage of the total number of synapses. Only micrographs from neurons stained for VGluT2 and VGAT, and with dendrites in SNc and SNr (*n* = 3) were included.

Proportions of varicosities immunopositive for VGluT1, VGluT2 and VGAT

Midbrain sections of three paraformaldehyde-fixed (4%) rats were immunostained to reveal VGluT2, VGAT and VGluT1 (1:1,000, monoclonal mouse antibody to VGluT1, MAb Technologies) using the ABC method essentially as described above. The number of varicosities immunopositive for each of the transporters in SNc and SNr were estimated by an unbiased procedure using the optical fractionator workflow in Stereo Investigator.

Contours for SNc and SNr were obtained from an adjacent Nissl-stained series. The counting frames (10×10 μm) were distributed randomly using a 100×60 μm grid over the SNc and a 250×150 μm grid over the SNr. For VGluT2 and VGAT, the optical fractionators had a 100 μm^2 surface and were 6 μm thick, with a guard zone of 1 μm. For VGluT1, the incidence of varicosities using these sampling parameters was near zero, so a (50×50 μm, or 2,500 μm^2) surface counting frame was used. For the VGluT1 series, we sampled (mean ± s.e.m.) 416.0 ± 115.5 and 79.3 ± 19.5 varicosities in the SNc and SNr, respectively ($n = 3$). For the VGluT2 series, we sampled 175.0 ± 59.0 and 150.3 ± 76.9 varicosities in the SNc and SNr, respectively ($n = 3$). For the VGAT series, we sampled 218.7 ± 155.6 and 334 ± 155.6 varicosities in the SNc and SNr, respectively ($n = 3$). The proportions for each marker are expressed as the percentage of all three presynaptic markers and are thus expected to be higher than in the electron microscopy analyses.

Statistical analysis

Descriptive (mean, s.e.m. and range), comparative (*t* test, one- or two-way ANOVA, repeated-measures two-way ANOVA) and correlative (Pearson's correlation) statistics were performed using SigmaPlot 11 or Sigmastat 3.5. Pairwise *post hoc* comparisons were performed using a Student-Newman-Keuls *post hoc* test (refer to SigmaPlot software for details). Data were assessed for normality using the single-sample Kolmogorov-Smirnov test, on which parametric statistics were used. Level of significance was set at 0.05.

Supplementary Material

Refer to Web version on PubMed Central for supplementary material.

Acknowledgments

References

1. Wise RA. Roles for nigrostriatal–not just mesocorticolimbic–dopamine in reward and addiction. Trends Neurosci. 2009; 32:517–524. [PubMed: 19758714]

2. Schultz W. Behavioral dopamine signals. Trends Neurosci. 2007; 30:203–210. [PubMed: 17400301]

3. Tsai HC, et al. Phasic firing in dopaminergic neurons is sufficient for behavioral conditioning. Science. 2009; 324:1080–1084. [PubMed: 19389999]

4. Blythe SN, Wokosin D, Atherton JF, Bevan MD. Cellular mechanisms underlying burst firing in substantia nigra dopamine neurons. J. Neurosci. 2009; 29:15531–15541. [PubMed: 20007477]

5. Kitai ST, Shepard PD, Callaway JC, Scroggs R. Afferent modulation of dopamine neuron firing patterns. Curr. Opin. Neurobiol. 1999; 9:690–697. [PubMed: 10607649]

6. Brischoux F, Chakraborty S, Brierley DI, Ungless MA. Phasic excitation of dopamine neurons in ventral VTA by noxious stimuli. Proc. Natl. Acad. Sci. USA. 2009; 106:4894–4899. [PubMed: 19261850]

7. Brown MT, Henny P, Bolam JP, Magill PJ. Activity of neurochemically heterogeneous dopaminergic neurons in the substantia nigra during spontaneous and driven changes in brain state. J. Neurosci. 2009; 29:2915–2925. [PubMed: 19261887]

8. Bromberg-Martin ES, Matsumoto M, Hikosaka O. Dopamine in motivational control: rewarding, aversive and alerting. Neuron. 2010; 68:815–834. [PubMed: 21144997]

9. Matsumoto M, Hikosaka O. Two types of dopamine neuron distinctly convey positive and negative motivational signals. Nature. 2009; 459:837–841. [PubMed: 19448610]

10. Joshua M, Adler A, Mitelman R, Vaadia E, Bergman H. Midbrain dopaminergic neurons and striatal cholinergic interneurons encode the difference between reward and aversive events at different epochs of probabilistic classical conditioning trials. J. Neurosci. 2008; 28:11673–11684. [PubMed: 18987203]

11. Tepper JM, Lee CR. GABAergic control of substantia nigra dopaminergic neurons. Prog. Brain Res. 2007; 160:189–208. [PubMed: 17499115]

12. Bolam JP, Francis CM, Henderson Z. Cholinergic input to dopaminergic neurons in the substantia nigra: a double immunocytochemical study. Neuroscience. 1991; 41:483–494. [PubMed: 1678502]

13. Bolam JP, Smith Y. The GABA and substance P input to dopaminergic neurones in the substantia nigra of the rat. Brain Res. 1990; 529:57–78. [PubMed: 1704287]

14. Lavoie B, Parent A. Pedunculopontine nucleus in the squirrel monkey: cholinergic and glutamatergic projections to the substantia nigra. J. Comp. Neurol. 1994; 344:232–241. [PubMed: 7915727]

15. Smith Y, Charara A, Parent A. Synaptic innervation of midbrain dopaminergic neurons by glutamate-enriched terminals in the squirrel monkey. J. Comp. Neurol. 1996; 364:231–253. [PubMed: 8788247]

16. Smith Y, Bevan MD, Shink E, Bolam JP. Microcircuitry of the direct and indirect pathways of the basal ganglia. Neuroscience. 1998; 86:353–387. [PubMed: 9881853]

17. Pinault D. A novel single-cell staining procedure performed *in vivo* under electrophysiological control: morpho-functional features of juxtacellularly labeled thalamic cells and other central neurons with biocytin or neurobiotin. J. Neurosci. Methods. 1996; 65:113–136. [PubMed: 8740589]

18. Ascoli GA. Mobilizing the base of neuroscience data: the case of neuronal morphologies. Nat. Rev. Neurosci. 2006; 7:318–324. [PubMed: 16552417]

19. Preston RJ, McCrea RA, Chang HT, Kitai ST. Anatomy and physiology of substantia nigra and retrorubral neurons studied by extra- and intracellular recording and by horseradish peroxidase labeling. Neuroscience. 1981; 6:331–344. [PubMed: 6164011]

20. Fallon, JH.; Loughlin, SE. Substantia nigra. In: Paxinos, G., editor. The Rat Nervous System. Academic Press; London: 1995. p. 215-238.

21. Gerfen CR, Baimbridge KG, Thibault J. The neostriatal mosaic. III. Biochemical and developmental dissociation of patch-matrix mesostriatal systems. J. Neurosci. 1987; 7:3935–3944. [PubMed: 2891800]

22. West MJ. Stereological methods for estimating the total number of neurons and synapses: issues of precision and bias. Trends Neurosci. 1999; 22:51–61. [PubMed: 10092043]

23. Gundersen HJ. Stereology of arbitrary particles. A review of unbiased number and size estimators and the presentation of some new ones, in memory of William R. Thompson. J. Microsc. 1986; 143:3–45. [PubMed: 3761363]

24. Naito A, Kita H. The cortico-nigral projection in the rat: an anterograde tracing study with biotinylated dextran amine. Brain Res. 1994; 637:317–322. [PubMed: 7514084]

25. Omelchenko N, Sesack SR. Glutamate synaptic inputs to ventral tegmental area neurons in the rat derive primarily from subcortical sources. Neuroscience. 2007; 146:1259–1274. [PubMed: 17391856]

26. Corvaja N, Doucet G, Bolam JP. Ultrastructure and synaptic targets of the raphe-nigral projection in the rat. Neuroscience. 1993; 55:417–427. [PubMed: 7690910]

27. Smith Y, Hazrati LN, Parent A. Efferent projections of the subthalamic nucleus in the squirrel monkey as studied by the PHA-L anterograde tracing method. J. Comp. Neurol. 1990; 294:306–323. [PubMed: 2332533]

28. Mann EO, Paulsen O. Role of GABAergic inhibition in hippocampal network oscillations. Trends Neurosci. 2007; 30:343–349. [PubMed: 17532059]

29. Fiala, JC.; Spacek, J.; Harris, KM. Dendrite structure. In: Stuart, GJ.; Spruston, N.; Hausser, M., editors. Dendrites. Oxford University Press; Oxford: 2008. p. 1-41.

30. Magee JC. Dendritic integration of excitatory synaptic input. Nat. Rev. Neurosci. 2000; 1:181–190. [PubMed: 11257906]

31. Comoli E, et al. A direct projection from superior colliculus to substantia nigra for detecting salient visual events. Nat. Neurosci. 2003; 6:974–980. [PubMed: 12925855]

32. Borgius L, Restrepo CE, Leao RN, Saleh N, Kiehn O. A transgenic mouse line for molecular genetic analysis of excitatory glutamatergic neurons. Mol. Cell. Neurosci. 2010; 45:245–257. [PubMed: 20600924]

33. Wang HL, Morales M. Pedunculopontine and laterodorsal tegmental nuclei contain distinct populations of cholinergic, glutamatergic and GABAergic neurons in the rat. Eur. J. Neurosci. 2009; 29:340–358. [PubMed: 19200238]

34. Iribe Y, Moore K, Pang KC, Tepper JM. Subthalamic stimulation-induced synaptic responses in substantia nigra pars compacta dopaminergic neurons *in vitro*. J. Neurophysiol. 1999; 82:925–933. [PubMed: 10444687]

35. Hajós M, Greenfield SA. Synaptic connections between pars compacta and pars reticulata neurones: electrophysiological evidence for functional modules in the substantia nigra. Brain Res. 1994; 660:216–224. [PubMed: 7820690]

36. Spruston N. Pyramidal neurons: dendritic structure and synaptic integration. Nat. Rev. Neurosci. 2008; 9:206–221. [PubMed: 18270515]

37. Megías M, Emri Z, Freund TF, Gulyas AI. Total number and distribution of inhibitory and excitatory synapses on hippocampal CA1 pyramidal cells. Neuroscience. 2001; 102:527–540. [PubMed: 11226691]

38. Grace AA, Bunney BS. Paradoxical GABA excitation of nigral dopaminergic cells: indirect mediation through reticulata inhibitory neurons. Eur. J. Pharmacol. 1979; 59:211–218. [PubMed: 527646]

39. Gulácsi A, et al. Cell type-specific differences in chloride-regulatory mechanisms and GABA(A) receptor-mediated inhibition in rat substantia nigra. J. Neurosci. 2003; 23:8237–8246. [PubMed: 12967985]

40. Paladini CA, Celada P, Tepper JM. Striatal, pallidal and pars reticulata evoked inhibition of nigrostriatal dopaminergic neurons is mediated by GABA(A) receptors *in vivo*. Neuroscience. 1999; 89:799–812. [PubMed: 10199614]

41. Jhou TC, Fields HL, Baxter MG, Saper CB, Holland PC. The rostromedial tegmental nucleus (RMTg), a GABAergic afferent to midbrain dopamine neurons, encodes aversive stimuli and inhibits motor responses. Neuron. 2009; 61:786–800. [PubMed: 19285474]

42. Mailly P, Charpier S, Menetrey A, Deniau JM. Three-dimensional organization of the recurrent axon collateral network of the substantia nigra pars reticulata neurons in the rat. J. Neurosci. 2003; 23:5247–5257. [PubMed: 12832549]

43. Maeda H, Mogenson GJ. Effects of peripheral stimulation on the activity of neurons in the ventral tegmental area, substantia nigra and midbrain reticular formation of rats. Brain Res. Bull. 1982; 8:7–14. [PubMed: 7055735]

44. Coizet V, Dommett EJ, Klop EM, Redgrave P, Overton PG. The parabrachial nucleus is a critical link in the transmission of short latency nociceptive information to midbrain dopaminergic neurons. Neuroscience. 2010; 168:263–272. [PubMed: 20363297]

45. Lodge DJ. The medial prefrontal and orbitofrontal cortices differentially regulate dopamine system function. Neuropsychopharmacology. 2011; 36:1227–1236. [PubMed: 21307842]

46. Bayer VE, Pickel VM. GABA-labeled terminals form proportionally more synapses with dopaminergic neurons containing low densities of tyrosine hydroxylase immunoreactivity in rat ventral tegmental area. Brain Res. 1991; 559:44–55. [PubMed: 1685938]

47. Paxinos, G.; Watson, C. The Rat Brain in Stereotaxic Coordinates. Elselvier; Amsterdam: 2007.

48. Bolam, JP. Experimental Neuroanatomy: a Practical Approach. IRL Press; Oxford: 1992.

49. Sadek AR, Magill PJ, Bolam JP. A single-cell analysis of intrinsic connectivity in the rat globus pallidus. J. Neurosci. 2007; 27:6352–6362. [PubMed: 17567796]
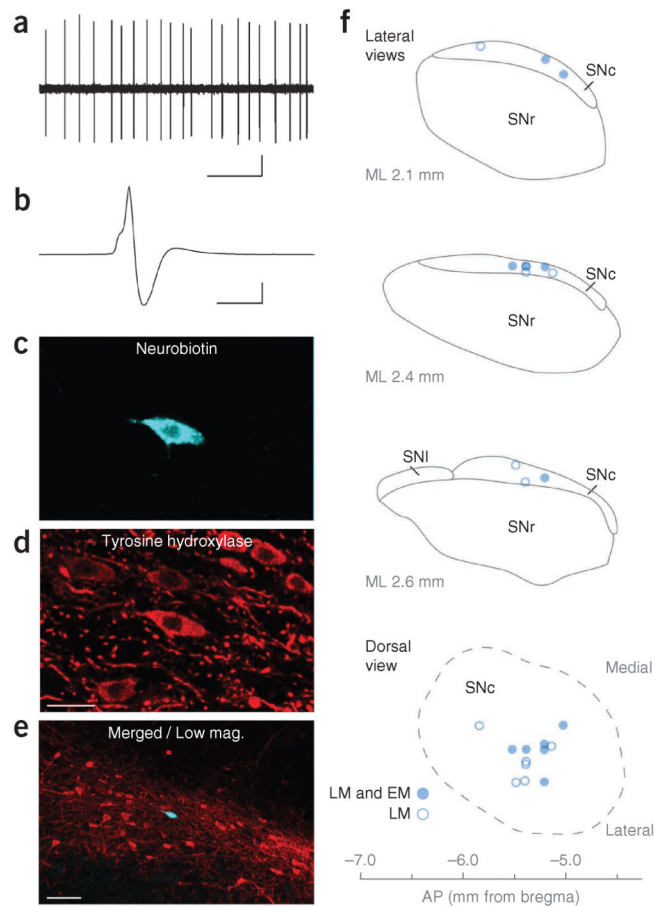
Figure 1. Recording and identification of SNc dopaminergic neurons.
(**a,b**) Spontaneous firing (**a**) and action potential waveform (average of 150 spikes, **b**) of a typical dopaminergic neuron *in vivo*. (**c-e**) The neuron was labeled with neurobiotin (cyan, **c**); it expressed tyrosine hydroxylase immunoreactivity (red, **d**), identifying it as a dopaminergic neuron, and was located in the SNc (merged image at low magnification, **e**). (**f**) Location of cell bodies of all of the dopaminergic neurons that we studied (six for light and electron microscopy (LM and EM) and six for light microscopy alone), in three lateral views (top) and one projected dorsal view (bottom). Scales bars represent 0.5 mV (vertical bars in **a** and **b**), 1 s (**a**), 2 ms (**b**), 20 μm (**c,d**) and 100 μm (**e**). AP, anteroposterior; ML, mediolateral; SNl, substantia nigra pars lateralis.
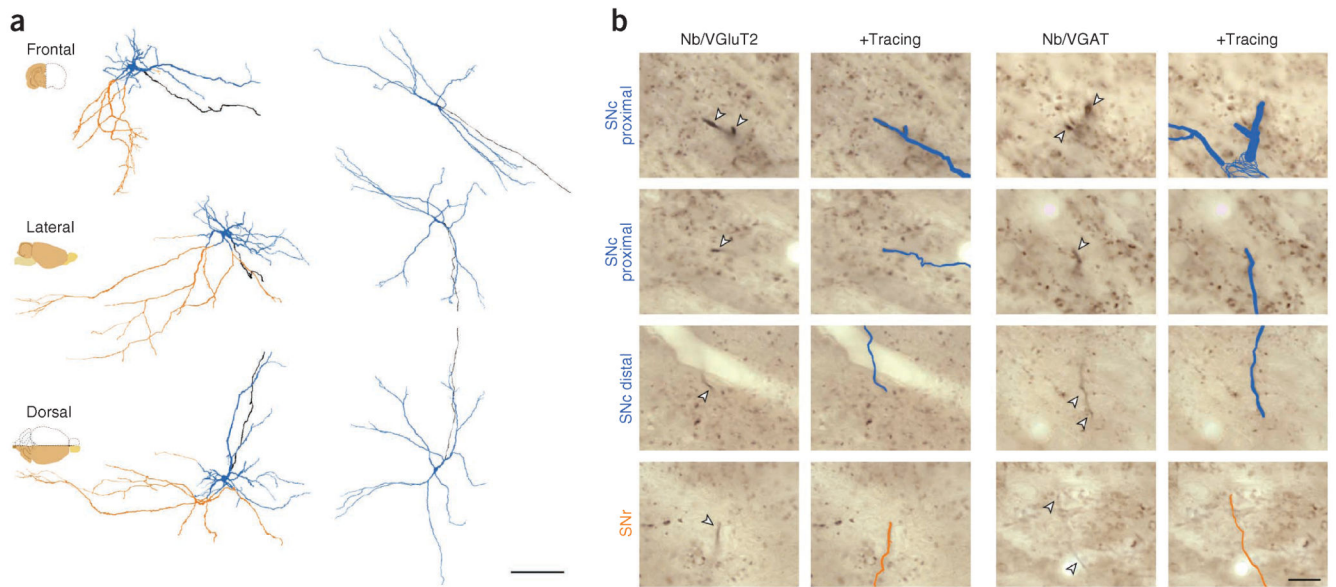
Figure 2. Three-dimensional digital reconstructions of identified SNc dopaminergic neurons.
(**a**) Two SNc dopaminergic neurons, as seen in different planes. Both have dendrites in the SNc (light blue), but the cell on the left also has dendrites in the underlying SNr (orange). Axons are shown in black. (**b**) Neurobiotin (Nb)-labeled dendrites (white arrowheads) located in SNc, as seen directly in the tissue sections or with the projected three-dimensional reconstruction overlaid (+Tracing, blue). Glutamatergic (VGluT2 immunopositive) and GABAergic (VGAT immunopositive) presynaptic terminals appear as lighter brown, punctuate labeling. Scale bars represent 200 μm (**a**) and 5 μm (**b**).
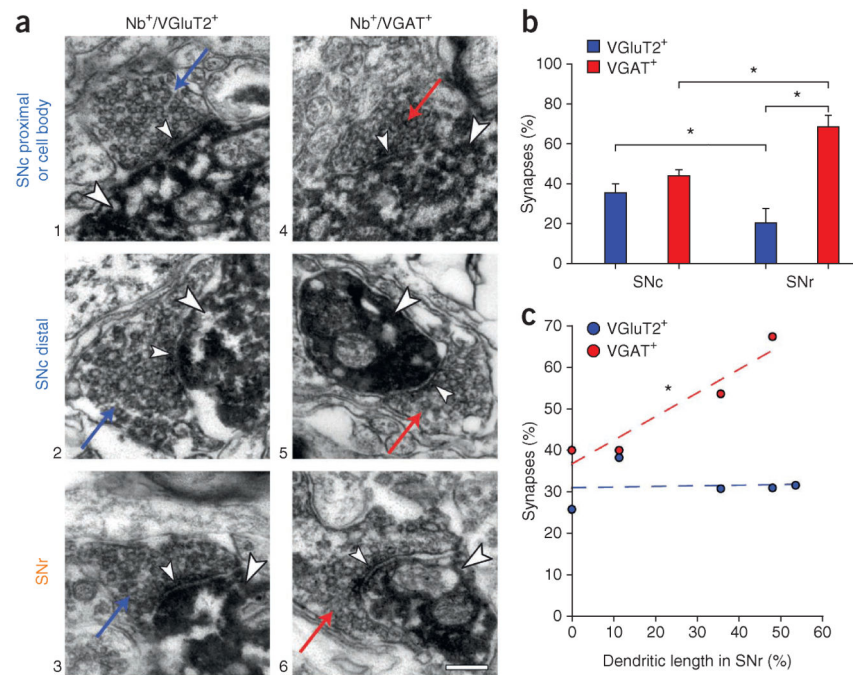
Figure 3. Proportions and localization of glutamatergic and GABAergic synapses made with individual dopaminergic neurons.

(**a**) Electron micrographs of glutamatergic (VGluT2^{+}, blue arrows) and GABAergic (VGAT[+], red arrows) axon terminals forming synapses (small arrowheads) with a neurobiotin-labeled (large arrowheads) cell body (4) and dendrites in SNc (1, 2 and 5) and SNr (3 and 6). Scale bar represents 200 nm. (**b**) The proportion of GABAergic (VGAT[+]) synapses made with dendrites located in the SNr was significantly greater than that of GABAergic synapses in SNc and glutamatergic synapses in the SNr, whereas the proportion of glutamatergic (VGluT2^{+}) synapses was significantly greater in the SNc than in SNr (mean ± s.e.m.). (**c**) The proportion of GABAergic synapses, but not glutamatergic synapses, was correlated with the proportion of total dendritic length in the SNr. Five neurons were analyzed for VGluT2^{+} synapses and four for VGAT[+] synapses. $*P < 0.05$.
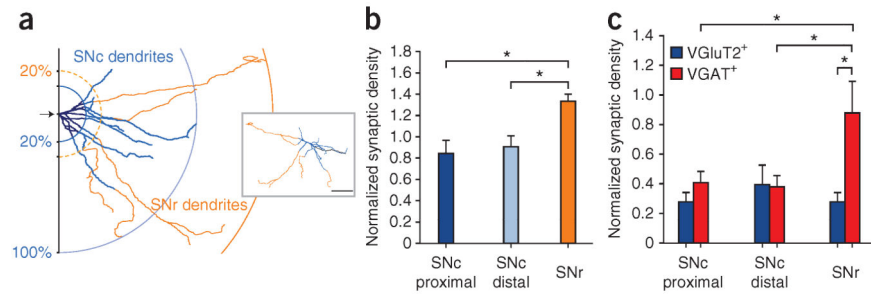
Figure 4. Densities of synapses made with different dendritic compartments.
(**a**) Fan diagram showing classification of an individual dopaminergic neuron's dendrites in SNc (light blue) and SNr (orange) into proximal and distal domains. Inset shows the neuron at low magnification. Scale bar represents 200 μm. (**b**) The relative density of synapses was greater for SNr dendrites than for distal or proximal SNc dendrites in individual neurons. (**c**) The relative density of GABAergic synapses (VGAT[+]) was greater for SNr dendrites than for distal or proximal dendrites in the SNc, and also greater than that for glutamatergic synapses (VGluT2^{+}) in the SNr (mean ± s.e.m. for **b** and **c**). *$P < 0.05$.
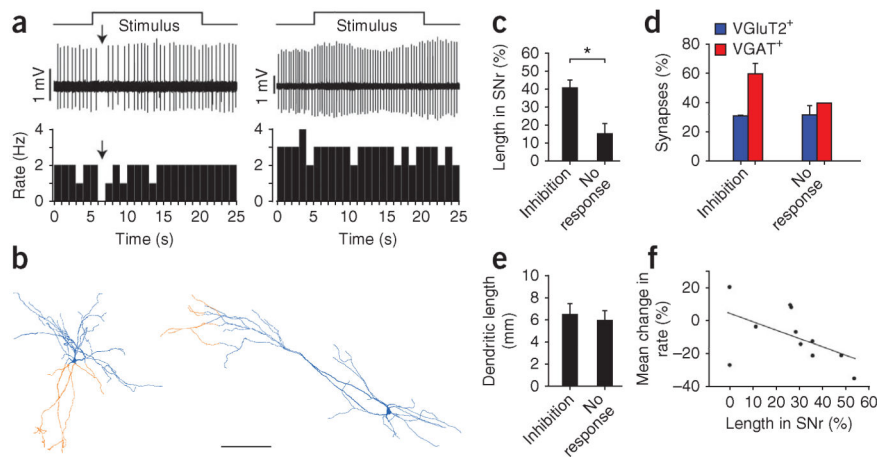
Figure 5. The responsiveness of individual dopaminergic neurons to aversive stimuli is correlated with the proportion of their dendrites located in SNr.
(**a**) Examples of a neuron inhibited (arrow) by a noxious stimulus (hind paw pinch) and another neuron that did not respond. (**b**) Digital reconstructions of the same neurons (left, lateral view; right, in frontal view). SNr dendrites are shown in orange and SNc dendrites in light blue. Note that a larger proportion of the dendrites of the inhibited neuron extended into SNr (orange) than those of the nonresponsive neuron. Scale bar represents 200 μm. (**c**) Neurons that were inhibited by the stimulus (inhibition group) had a significantly greater proportion of their dendrites in the SNr compared with the no response group. *$P < 0.05$. (**d**) Inhibited neurons had a greater proportion of GABAergic (VGAT+) synapses on their dendrites than did nonresponsive neurons. The proportions of glutamatergic (VGluT2+) synapses were similar for both groups. Five neurons were analyzed for VGluT2+ synapses (three inhibited, two no response) and four of them for VGAT+ synapses (two inhibited, two no response). (**e**) Inhibited and nonresponsive neurons were not significantly different in size, as measured in terms of total dendritic length (or number of dendritic segments or baseline firing rates before the stimulus delivery). (**f**) Mean percentage change in firing rate following the stimulus showed a negative correlation with the proportion of dendrites in SNr such that larger proportions of dendrites in SNr of dendrites were associated with larger decreases in rate ($R = -0.52$, $P = 0.052$, Pearson's product moment correlation). The data in **c, e** and **f** were derived from 11 neurons analyzed at the light microscopy level; five were significantly inhibited and six were not responsive (mean ± s.e.m. for **c-e**).

Table 1

Estimates of synapses made with SNc-located and SNr-located dendrites of individual SNc dopaminergic neurons

	Mean	S.e.m.	Range
All synapses (n = 6 neurons)			
Total number of synapses on neuron	8,063	851	5,152–10,908
% of all synapses on SNc dendrites	61.8	11.3	30–100
% of all synapses on SNr dendrites	38.2	11.3	0–70
VGluT2+ synapses (n = 5 neurons)			
On the entire neuron			
Total number of synapses	7,155	453	5,704–8,390
% of synapses VGluT2+	31.5	2.0	26–38
On the SNc dendrites			
Total number of synapses	4,859	422	3,643–5,704
% of synapses VGluT2+	35.4	4.3	26–48
On the SNr dendrites			
Total number of synapses	2,870	808	1,395–4,747
% of synapses VGluT2+	20.1	7.3	0–35
VGAT+ synapses (n = 4 neurons)			
On the entire neuron			
Total number of synapses	8,050	1,957	4,600–12,880
% of synapses VGAT+	50.2	6.5	40–67
On the SNc dendrites			
Total number of synapses	5,796	2,014	3,312–11,776
% of synapses VGAT+	43.7	3.0	38–50
On the SNr dendrites			
Total number of synapses	3,005	1,548	1,104–6,072
% of synapses VGAT+	68.5	5.5	60–79

Table 2

Absolute density of synapses made with individual SNc dopaminergic neurons

Synaptic density (synapses per μm^2)	Mean	S.e.m.	Range
All synapses (n = 6 neurons)			
Entire neuron	0.53	0.06	0.32–0.65
Proximal SNc dendrites	0.44	0.09	0.18–0.71
Distal SNc dendrites	0.51	0.07	0.36–0.73
SNc dendrites, total	0.47	0.06	0.25–0.59
SNr dendrites	0.73	0.12	0.40–0.93
VGluT2+ synapses (n = 5 neurons)			
Entire neuron	0.16	0.02	0.10–0.23
Proximal SNc dendrites	0.19	0.06	0.05–0.32
Distal SNc dendrites	0.15	0.04	0.04– 0.29
SNc dendrites, total	0.16	0.02	0.11–0.25
SNr dendrites	0.12	0.05	0.00–0.23
VGAT+ synapses (n = 4 neurons)			
Entire neuron	0.31	0.06	0.17–0.46
Proximal SNc dendrites	0.21	0.07	0.00–0.30
Distal SNc dendrites	0.26	0.06	0.14–0.41
SNc dendrites, total	0.23	0.03	0.17–0.30
SNr dendrites	0.58	0.13	0.44–0.85

Absolute density is calculated as the number of estimated synapses per μm^2 of approximate surface area of different somatodendritic compartments of dopaminergic neurons, as obtained from digital reconstructions using light microscopy (see Online Methods).